

EMC2

AD-A257 943

<rb1.t3; vers3.0; 12/18/91>



2

Electron Current, Beta Limit Line Operation and Power Balance in WB Model†

Robert W. Bussard and Katherine E. King

EMC2-0891-02

S **DTIC**
ELECTE
NOV 23 1992
A **D**

APPROVED FOR PUBLIC RELEASE
DISTRIBUTION UNLIMITED

CLEARED
FOR OPEN PUBLICATION

OCT 9 - 1992 3

STANDARD FOR FREEDOM OF INFORMATION
AND SECURITY REVIEW (CASD-PA)
DEPARTMENT OF DEFENSE

This document has been approved
for public release and sale, its
distribution is unlimited.

REVIEW OF THIS MATERIAL DOES NOT IMPLY
DEPARTMENT OF DEFENSE ENDORSEMENT OF
FACTUAL ACCURACY OR OPINION.

† This work performed under Contract No. MDA-972-90-C-0006 for
the Defense Advanced Research Projects Agency, Defense Sciences Office.

423136

92-29997



2888

EMC2® ENERGY/MATTER CONVERSION CORPORATION
9100 A Center Street, Manassas, VA 22110, (703) 330-7990

92-5-4384

ONE QUALITY INEPTORND 4.

Analysis of electron flow in the outer regions of the Polywelltm system shows the current required to achieve electron $\beta = 1$ at $r = R$ (the $\langle r_b \rangle = 1$ condition). This is found to depend on the square root of the injection energy, E_o , thus the $\langle r_b \rangle = 1$ power required will vary as $(E_o)^{1.5}$. With this as the drive power an expression for gross power gain, G_{gr} , can be obtained from the ratio of fusion power (integrated over system volume) to drive power. G_{gr} is calculated for several fuels. Each fuel combination has unique bremsstrahlung radiative characteristics. The inclusion of bremsstrahlung losses decreases the overall gain, G_{oa} , that can be attained by any system to values less than G_{gr} , and the maximum possible value for G_{oa} is found to be $G_{gr}/2$. The overall gain is derived and numerical and graphical examples are given to show the parametric range of system performance with such losses.

Results show that DT is superior and easily able to produce high gain in small systems (e.g. $R < 1.0$ m). It is also found that DD and D^3He tend to give comparable performance for comparable mixture ratios (0.25 – 0.5), and that both are considerably worse (ca. 10 – 100x)* than DT and better (10 – 100x) than $p^{11}B$. However, D^3He is seen to be no better than $p^{11}B$ if operated at mixture conditions that make it as non-hazardous (radiation-free) as $p^{11}B$. These analyses suggest that there is little incentive for use of D^3He in Polywelltm systems. They also show that $p^{11}B$ CAN be made to operate at net power, if core electron energies can be kept sufficiently low (small anode height) in contrast to conventional magnetic confinement systems, in which $p^{11}B$ can NOT be made to yield net power (vs. bremsstrahlung) under any conditions.

* The measure of "goodness" used here is the functional $F_{BR} = (B_o R)^4 / r_c$ (see later text).

Electron Current Flow at Surface $\beta = 1$ Conditions

Consider a system operating such that electron $\beta = 1$ at all times at the edge of the device, thus $\langle r_b \rangle = (r_b/R) = 1$. At this condition the parameters $Z = 8\pi n_c r_c^2$ and $W = E_o/(B_o R)^2$ are related by $(ZW) = 1$.¹ To calculate the electron injection current required to drive the device to and at this condition it is necessary first to know the electron density $n_e(R) = n_R$ at the system edge $r = R$.

The electron and ion charge densities are essentially equal throughout the body of the device, out to that radius² r_k at which the surface (edge) "sheath" begins.^{1*} At this position the ion density and electron density both increase with increasing $r \rightarrow R$, but the electron density increases more rapidly than the ion density. From the core radius $r = r_c$ to $r = r_k$ the density of both species varies closely as the inverse square $n(r) = n_c (r_c/r)^2$ so that the density of electrons at $r = r_k$ is given (approximately, see ref. 2) by $n(r_k) = n_k = n_c (r_c/r_k)^2$.

The total radial electron current at r_k is

$$I_{erk} = 4\pi r_k^2 n_k v_k \quad (1)$$

where v_k is the electron radial speed at r_k . The radial current at the surface at $r = R$ must be less than this, because conservation of magnetic moment and associated transverse momentum in the electron flow forces an increase in transverse electron kinetic energy with increasing radius beyond r_k (as well as an increase inside of r_k to the "stagnation radius"

^{1*} This radial position is that at which the kinetic energies of radial motion of ions and electrons are approximately equal (see e.g. ref. 2)

r_f), and thus a decrease in radial electron energy and hence in radial current at the boundary. This is accounted for here by a functional factor $F_e(f_{\perp}, \langle r_k \rangle) \leq 1$ that depends on the degree of transverse flow of the electrons. Thus the two currents can be related by

$$I_{eR} = I_{erk} F_e = 4\pi R^2 n_R v_R = 4\pi r_k^2 n_k v_k F_e \quad (2)$$

Now, for operation at $\langle r_b \rangle = 1$, there is no mirror reflection effect and the electron energy will simply follow the shape of the internal potential well which, in turn, will follow that of the internal B field. This will follow the functional form of the original unperturbed field, even though the field is at reduced amplitude due to the diamagnetic current reduction of field strength by the factor $f_D = B_{dia}/B_o(r)$ within the wiffle ball (WB) surface.³ With this shape, it can be shown that the total electron kinetic energy follows the formula¹

$$E_k(\langle r \rangle) = E_o \langle r \rangle^m f_o(\langle r \rangle) \quad (3)$$

for a rollover field of index exponent (m). For a truncated cube $m = 3$, the rollover function is $f_o = 2/(1 + \langle r \rangle^5)$, and thus the velocities vary about as $v(\langle r_k \rangle) = v(1)[2\langle r_k \rangle^3/(1 + \langle r_k \rangle^5)]^{0.5}$.

The functional factor F_e has been derived previously⁴ in terms of the "stagnation radius" r_f for electron flow in the outer regions of the system, where electrons establish the potential well that accelerates the ions. Adjusting this to the "critical radius" r_k by a correction term for the difference in potential and throughflow area between the stagnation radius $\langle r_f \rangle = (dE_{\perp}/E_o)^{0.5} = (f_{\perp})^{0.5}$ and the critical radius $\langle r_k \rangle$ at which the ion and electron density gradients change sign, and taking account of diamagnetic field reduction within the WB surface, gives this as approximately

$$F_e(f_{\perp}, \langle r_k \rangle) = \frac{\frac{\langle r_k \rangle^2}{f_{\perp}} \sqrt{\frac{f_D(1 - \langle r_k \rangle^3 f_o)}{f_D(1 - f_{\perp})}}}{\left[\sqrt{\frac{2 - f_{\perp}}{f_{\perp}}} - 1 \right] 3 \text{LN} \left[\frac{1}{\langle r_c \rangle} \right]} \quad (4)$$

Note that the diamagnetic factor f_D cancels out of the numerator of eq. (4); it is shown simply for completeness of description. With this, and including the multiplying effect of electron recirculation by the factor G_j , the surface electron injection current is then simply

$$I_{eR} = 4\pi R^2 n_c \langle r_c \rangle^2 v_R \left[f_o \langle r_k \rangle^3 \right]^{0.5} \left[\frac{F_e}{G_j k_s} \right] \quad (5)$$

for $\langle r_b \rangle = 1$ ($r = R$), where $k_s = 6.28E18$ chgs/Asec converts to current I_e in amps, the injection speed^{2*} of electrons is $v_R = (2E_o/m_e)^{1/2}$, and all units are cgs.

^{2*} Note that this speed is that at which the electrons are initially injected purely radially, while the actual electron motion at and near the boundary of the device, after the first pass through the system, will be very tangential due to the conservation of transverse momentum and of magnetic moment in electron flow through the multicusp system, as mentioned earlier. The functional factor F_e corrects for this use of a "false" radial speed at $r = R$. Note that this situation holds true for $\beta = 1$ operation out to any radius, as beyond or directly "at" the $\beta = 1$ radius the external B field is still imposed at its original strength, and the electrons will still "mirror" and conserve momentum through the magnetic moment effect in these regions, as well as inside the WB sphere if enough residual field is left therein. Finally, it is important to note that operation at $\beta = 1$ will almost certainly be cut off at $r = r_k$, due to the β instability beyond this radius, thus the region between r_k and R will still act in an MR mode fashion.

Electron Injection Power on the $\langle r_b \rangle = 1$ Line

Taking $(ZW) = 1$ on the $\langle r_b \rangle = 1$ line and noting that $G_j = 2r_e Z / N(k_L S)^2(1-\alpha_R)$ here and $Z = 8\pi r_e^2$, allows reduction of eq. (5) to yield

$$I_{eR} = \frac{(f_o \langle r_k \rangle^3 k_e)^{0.5} N(k_L S)^2(1-\alpha_R)}{(2m_e)^{0.5} (2r_e k_s)} (F_e)(E_o)^{0.5} \quad (6)$$

Here $r_e = 2.828E-13$ cm is the electron Compton radius, N is the effective cusp number, k_L is the effective loss radius factor³ (on surface gyro radius), S^2 is the average sine of the electron collision angle with the remaining cusp field at the adiabaticity radius, $\alpha_R = \alpha_g N_g / N$ is the effective repeller effectiveness α_r for N_g guns each with $\alpha_r = \alpha_g$, and $k_e = 1.6E-12$ ergs/eV allows E_o to be used in units of eV.

As an example, consider a truncated cube system with typical values of $f_{\perp} = 0.3$ (wide divergence of electrons), $\langle r_k \rangle = 0.83$ and $\langle r_e \rangle = 1E-2$. With these, the functional factor to correct for inertial flow convergence and magnetic and transverse momentum conservation effects becomes $F_e = 0.0610$. With this, and taking $N = 8.0$, $N_g = 6$ with $\alpha_g = 0.9$, $k_L = 2.0$ and $S^2 = 0.6$ (mean of range from $\pi/6$ to $2/3$),⁵ the electron drive current required is found to be related to the injection energy by

$$I_{eR} = 2.88(E_o)^{0.5} \quad (7)$$

for operation along the $\langle r_b \rangle = 1$ line. Here E_o is in eV.

Thus if $E_o = 1E4$ eV, for example, the drive current must be $I_{eR} = 288$ A; if $E_o = 2.5E4$ eV (25 keV), then $I_{eR} = 455$ A.

The $\langle r_b \rangle = 1$ line can be reached most directly by approaching WB mode operation from a small value of G_j (e.g. along the line of $G_{jwb} = 1$), starting operation at small current and increasing current until $\langle r_b \rangle = 1$ is attained. This requires that

$$G_{jwb} W = \frac{G_{jwb} E_o}{(B_o R)^2} = \frac{2r_e}{N(k_L S)^2} \quad (8)$$

Using this in eq. (6) shows that the critical injection current at $G_j = 1$ is related to the system field strength and size by

$$I_{eR} = \left[\frac{N}{r_e m_e} f_o \langle r_k \rangle^3 \right]^{0.5} \frac{k_L S (1 - \alpha_R)}{2k_s} F_e(B_o R) \quad (9)$$

For the previous parameters this becomes $I_{eR} = 0.39(B_o R)$ A, so that the field, size and injection energy are related by $(B_o R) = 7.37(E_o)^{0.5}$. For $R = 92$ cm, for example, this yields $B_o = 8.01$ G for $E = 1E4$ eV, $I_{eR} = 288$ A as illustrated above, or directly from eq. (8). At this condition the parameter $W = W_1 = 0.9064E-13$ cm, or $W_1 = 56.65$ keV/(kGcm)².

For $E_o = 1E4$ eV, as before, $P_{eR} = 2.88$ MW is required along the $\langle r_b \rangle = 1$ line. Having reached this line at $G_{jwb} = 1$ it is then possible to move up along this line by reducing the value of W from that at W_1 to successively lower values, keeping the injection current constant (or very nearly so). On this line G_{jwb} will vary inversely with W ; thus raising the B field by 10x will increase G_{jwb} by 100x, and increase Z by 100x.

Finally, note that this point ($G_{jWB} = 1$, $\langle r_b \rangle = 1$) and the $\langle r_b \rangle = 1$ line can be attained only by injection of the required current at an electron drive power of

$P_{eR} = 2.88(E_o)^{1.5}$ watts. Any system to produce net power with these parameters must operate with more than 2.88 MW of fusion power generation.

Fusion Power Generation and Gross Gain

The fusion power output is given as the core-generated power multiplied by a correction factor, K_f , in the approximate algorithmic form

$$P_{fus} = \left[\frac{4\pi r_c^3}{3} \right] (K_f) (n_i^2 \sigma_{fo} [E_o(1-\eta)]^s) (E_f) \frac{k_e^{1.5}}{10} \left[\frac{2E_o(1-\eta)}{\bar{m}_i} \right]^{0.5} b_{ij} \quad (10)$$

Here the factor $K_f = 2(1-\eta_o)/(1-\eta)$ accounts for the fact that up to 0.75–0.85 of the power is generated outside the convergence-limited core at radius r_c , depending upon the anode height, η .⁶ Here the fusion cross-section has been taken, for illustrative purposes, to be $\sigma_{fus} = \sigma_{fo} E_o^s$ over the energy range of interest.⁴ This simple formulation allows analytical illustration of the relationships between fuel properties, system parameters, and system gross gain. More exact cross-section formulae are used later for computer calculations of these relationships. Recalling that $n_c = n_1 Z_1 + n_2 Z_2$, where $n_1 = f_1 n_i$ and $n_2 = f_2 n_i$,⁷ the core density is found from the identities $ZW = 1$, $Z = 8\pi n_c r_c^2$ and W from eq. (8), to be

$$n_i = \left[\frac{N(k_L S)^2 G_{jwb}}{2r_e 8\pi r_c^2} \right] \frac{1}{1+f_2(Z_2-1)} \quad (11)$$

With this the fusion power becomes

$$P_{fus} = \frac{b_{ij} K_f \sigma_{fo} E_f (2/\bar{m}_i)^{0.5} [E_o(1-\eta)]^{s+0.5} (k_L S)^4 (k_e)^{1.5} (N^2)}{3 \times 64 \times 10\pi (r_e)^2 r_c [1+f_2(Z_2-1)]^2} (G_{jwb})^2 \quad (12)$$

Since $G_{jwb} = W_1/W = (B_o/B_1)^2$ for W_1 taken at $G_{jwb} = 1$, $\langle r_b \rangle = 1$, it is evident that P_{fus} scales as B_o^4 . Note that this is the same as and directly analogous to the power scaling of all other magnetic confinement fusion concepts. The power amplification or gross power gain G_{gr} is this expression eq. (12) divided by $I_{eR} E_o$ from eq. (6), or

$$G_{gr} = \frac{b_{ij} k_s k_e (m_e / \bar{m}_i)^{0.5} (K_f \sigma_{fo} E_f N) (k_L S)^2 (E_o)^{s-1} (1-\eta)^{s+0.5}}{(f_o \langle r_k \rangle^3)^{0.5} (480 \pi r_e r_c) F_e [1 + f_2 (Z_2 - 1)]^2 (1 - \alpha_R)} (G_{jwb})^2 \quad (13)$$

for E_f in MeV and E_o in eV, with all other units in cgs, but $\sigma_{fo} = \text{cm}^2/(\text{eV})^s$.

For DT fuel $E_f = 17.6$ MeV and $b_{ij} = 0.25$ (for 50:50 mixtures). At $E_o = 2E4$ eV (20 keV), the fusion reaction cross-section varies about as $s = 2.7$ with a coefficient given approximately as $\sigma_{fo} = 3.5E-36 \text{ cm}^2/(\text{eV})^{2.7}$. Taking $\eta = 0.1$, \bar{m}_i (reduced) = $1.2 m_p$ and $r_c = 1.0$ cm, and other parameters as before, eq. (13) gives

$$G_{gr}|_{DT} = 2.60E-10 (G_{jwb})^2 \quad (14)$$

Thus net power can be made only if $G_{jwb} > 6.2E4$. For $p^{11}B$ (50:50, with $\bar{m}_i = 0.9 m_p$) at 300 keV ($s = 2.85$, $\sigma_{fo} = 4.48E-41 \text{ cm}^2/(\text{eV})^{2.85}$) it is similarly found (for $r_c = 1.0$ cm) that

$$G_{gr}|_{p^{11}B} = 1.76E-13 (G_{jwb})^2 \quad (15)$$

so that net power requires that $G_{jwb} > 2.4E6$. For a system gross power gain of $G_{gr} = 40$ with DT, $G_{jwb} > 3.93E5$, while for $p^{11}B$, $G_{jwb} > 1.51E7$, for the parameters chosen in the foregoing examples.

It is instructive to restate these gross gains in terms of the system size and fields required. To do this, return to eq. (8) and write G_{jwb} in terms of $(B_o R)$ and E_o , and substitute into eqs. (13,14,15), thus

$$G_{gr} = \left[\frac{k_s r_e}{k_e} \right] \frac{(m_e/\overline{m}_i)^{0.5} (b_{ij} K_f \sigma_{fo} E_f) (E_o)^{s-3} (1-\eta)^{s+0.5}}{(f_o < r_k >^3)^{0.5} (120\pi r_c) (N) (k_L S)^2 F_e [1+f_2(Z_2-1)]^2 (1-\alpha_R)} (B_o R)^4 \quad (16)$$

and

$$G_{gr}|_{DT} = 0.022 E-20 (B_o R)^4 / r_c \quad (17a)$$

for B_o in gauss (G), R and r_c in cm, or

$$G_{gr}|_{DT} = 0.022 (B_o R)^4 / r_c \quad (17b)$$

for B_o in kG, R and r_c in m. For example, for $<r_c> = 0.01$, if $R = 0.5$ m, $B = 4.5$ kG, then $G_{gr} = 1.13$; if $R = 0.8$ m, $B = 8.0$ kG, then $G_{gr} = 46.1$. And for $p^{11}B$ at the previous conditions

$$G_{gr}|_{p^{11}B} = 0.066 E-26 (B_o R)^4 / r_c \text{ (cgs)} \quad (18a)$$

$$G_{gr}|_{p^{11}B} = 0.066 E-6 (B_o R)^4 / r_c \text{ (kG, m)} \quad (18b)$$

Thus, for $<r_c> = 0.01$, if $B_o = 15$ kG then $R = 8.0$ m is needed for $G_{gr} = 1.14$. If $B_o = 25$ kG and $R = 10.0$ m, then the gross gain can be $G_{gr} = 17.2$.

Note from eq. (16) that G_{gr} will increase with increasing E_o only if the fusion cross-section changes more rapidly than $s = 3$. Since p^6Li and DD reactions (as well as some others) have $s < 3$ over most of their energy range of interest, it is clear that high energy operation is not necessarily optimal for use of such fuels.

Bremmstrahlung Losses and System Overall Gain in $\langle r_b \rangle = 1$ Mode

However, the above gain formula (eq. 16) does not account for bremsstrahlung losses. If these are included it is found that low energy operation leads to excessive bremsstrahlung vs. fusion power density. There is thus an optimum value for well depth (mean reaction energy) for any fuel combination with $s < 3$. In the region where cross-section variation is $s \geq 3$, there is no optimum well depth driven by bremsstrahlung, and the best well depth is that at the highest possible cross-section for $s > 3$, so long as the core electrons remain cold. Calculating bremsstrahlung power as core-generated radiative power multiplied by a correction factor K_b , for extra-core bremsstrahlung (as for fusion power), the fusion/bremsstrahlung power ratio is given from eq. (10) and the standard formulae for core bremsstrahlung emission,⁷ evaluated at core conditions, as

$$\langle P_{fb} \rangle = \frac{K_f (\sigma_{fo} E_f E_o^s) (1-\eta)^{s-0.5} (2/\overline{m}_i)^{0.5} b_{ij} k_e^{1.5}}{1.69e-31 K_b F_z \eta_e^{0.5}} \quad (19)$$

where $F_z = [1+f_2(Z_2-1)][1+f_2(Z_2^2-1)]$. The factor K_b is found to be approximately 2.5 for most systems of interest. With this, the system overall gain (G_{oa}), including bremsstrahlung losses (but not including ohmic power to drive the magnetic field coils), will be

$$G_{oa} = \frac{1}{\frac{1}{G_{gr}} + \frac{1}{\langle P_{fb} \rangle}} \quad (20)$$

Writing $G_{gr} = C_e(E_o)^{s-3}$ (from eq. 16) and $\langle P_{fb} \rangle = C_b(E_o)^s$ (from eq. 19) and differentiating eq. (20) to find the optimum condition for E_o for those fuels with $s < 3$ yields

$$E_o|_{opt} = \left[\frac{sC_e}{(3-s)C_b} \right]^{1/3} \quad (21)$$

and if $s = 1.50$, for example (a reasonable fit to several of the fusion reactions over the midrange of their ascending cross-section energy region), then $E_o|_{opt} = (C_e/C_b)^{1/3}$ and the overall gain eq. (20) gives the maximum possible gain as

$$G_{oa}|_{max} = \frac{\sqrt{C_e C_b}}{2} \quad (22)$$

For $s = 1.50$, eqs. (20) and (21) require that $G_{gr} = \langle P_{fb} \rangle$ at optimum operation. At this condition eq. (22) shows that $G_{oa}|_{max} = G_{gr}/2$ is the largest possible overall gain of the system. Thus, the maximum performance of a fuel with $s = 1.5$ will be set by the value of $F_{BR} = (B_o R)^4 / r_c = B_o^4 R^3 / \langle r_c \rangle$; larger values of $(B_o R)$ give higher values of G_{oa} . All cross-sections eventually reach a peak with increasing energy, at which point $s = 0$. Thus as the reaction energy (well depth) is increased above the region where $s = 1.5$, this exponent decreases steadily to $s = 0$, and becomes negative thereafter. At energies above the $s = 1.5$ region, the σ_f/E_o^3 term decreases more and more rapidly and the effect of increasing F_{BR} becomes less and less until, as σ_f approaches its peak value, increasing F_{BR}

has no effect at all. This behavior is seen quite clearly in graphic portrayals of these parameter variations.

These can be obtained from the foregoing analyses in considerably improved form by use of correct functional formulae for the fusion cross-sections of the various candidate fuels. For convenience these are summarized in Table 1, for several fuels. The table gives the cross-section variation with mean collision energy in the CM/CG system that characterizes these Polywelltm converging-flow systems. Using the functional form $\sigma_f(E)$, where $E = E_o(1-\eta)$, and letting $\alpha_R = 0$, recasts eq. (16) as

$$G_{gr} = \frac{(k_s r_e / k_e) [(1-\eta) m_e / \bar{m}_i]^{0.5} (b_{ij} K_f E_f) [\sigma_f(E)]}{(f_o <r_k>^3)^{0.5} (120\pi <r_c>) (E_o)^3 (N) (k_L S)^2 F_e [1+f_2(Z_2-1)]^2} (B_o^4 R^3) \quad (23)$$

Figures 1(a-d) show the parameter G_{gr}/F_{BR} , where $F_{BR} = (B_o R)^4 / r_c$, as a function of electron injection energy E_o , with $f_1 = 0.3$, for the fuels in Table 1, for several values of the anode height parameter η and a core convergence ratio of $<r_c> = 0.01$, for equal fractional mixtures of fuel components, $f_1 = f_2 = 0.5$ ($f_1 + f_2 = 1.0$), where f_1 is the fractional mix of singly-ionized ($Z = 1$) fuel and f_2 is that of the multiply-ionized ($Z > 1$) fuel component.

Figures 1(e-h) show G_{gr}/F_{BR} for fuel fraction f_2 at optimum values to yield the maximum ratio of fusion to bremsstrahlung power, taken from prior study of bremsstrahlung losses.⁷ These are $f_2 = 0.261$ for D^3He , 0.084 for $p^{11}B$ and 0.5 for DT. The curves for DT and DD are, of course, identical in both sets of figures. Note that DD surpasses D^3He in gross gain performance, that DT is clearly best, and $p^{11}B$ most difficult and least promising.

The value of G_{gr} scales simply with $\langle r_c \rangle$ as $G_{gr} = G_{gr}^* (10^{-2} / \langle r_c \rangle)$ where G_{gr}^* is the gross gain value as shown in Figures 1. It is interesting to note the position of the maxima for the different fuels. Increasing anode height results in lower values of gross gain, and shifts the peak to slightly higher E_0 values. Also note that the gross gain for D^3He and $p^{11}B$ is only slightly improved at optimum bremsstrahlung mixture ratio than for 50:50 mixtures.

Use of this equation together with eq. (19) for bremsstrahlung allows exact computation of the overall gain including bremsstrahlung G_{oa} from eq. (20). This is shown in Figures 2-5 as a function of E_0 for each fuel, for a range of the parameter F_{BR} , and for two values of the minimum core electron energy (anode height), $\eta_e = \eta$, of 0.01 and 0.1. The bremsstrahlung extra-core factor was taken to be $K_b = 2.5$ in these calculations.

Figures 2(a,b) and 3(a,b) show overall gain for DT and DD, respectively, for $f_1 = f_2 = 0.5$ mixtures at two values of $\eta_e = \eta$. Note that the position of maximum G_{oa} has shifted upward in energy very slightly for DT, but up by as much as 10x for DD; a result of the weak energy dependence of the DD fusion cross-section to counter balance bremsstrahlung losses.

Figures 4(a-d) and 5(a-d) show G_{oa} for D^3He and $p^{11}B$, respectively, for 50:50 mixtures (Figs. a,b) and bremsstrahlung-optimum- f_2 mixtures (Figs. c,d) at two values of $\eta_e = \eta$. For both fuels the gain is increased and the peak injection energy required is higher at the optimum f_2 value. The effect with $p^{11}B$ is more pronounced than for D^3He , and it is clear that $p^{11}B$ can give net power only at small values of $\eta < 0.03$, no matter how large F_{BR} may be made.

As an example of the situation consider a $p^{11}\text{B}$ system operating at $E_0 = 500 \text{ keV}$ with $G_{\text{oa}} = 7.9$ at $F_{\text{BR}} = 1\text{E}11 = (B_0 R)^4 / r_c$. If $\langle r_c \rangle = 1\text{E}-3$, for example, the $B_0^4 R^3 = 1\text{E}8 (\text{kG})^4 (\text{m}^3)$. Thus, if $B_0 = 31.6 \text{ kG}$, $R = 4.64 \text{ m}$ is required, or if $R = 2.5 \text{ m}$, then $B_0 = 50.3 \text{ kG}$ must be supplied. These are large parameters by the standards of the small systems attainable with DT, but still small compared with magnetic confinement fusion systems. The fact that $p^{11}\text{B}$ can be made to yield net power is a result of the unique energy and particle distributions inherent in the Polywelltm inertial-electrostatic system. This useful result is in striking contrast to all conventional magnetic confinement systems, where $p^{11}\text{B}$ can not be made to work at all.

Comparison of DD and D^3He shows that the two offer comparable performance (G_{oa}) at $F_{\text{BR}} = 1\text{E}8$ but that the overall gains for D^3He become larger than those for DD at $F_{\text{BR}} > 1\text{E}8$; a factor of 3x higher at $F_{\text{BR}} = 1\text{E}9$. However, the injection energy (well depth) is about 2x higher at this latter condition.

Finally, while it is clear that D^3He offers much higher performance than $p^{11}\text{B}$ for the mixtures assumed, at smaller values of both E_0 and F_{BR} , it is important to note that this performance includes a very large neutron production rate and consequent radiation hazard, not present with $p^{11}\text{B}$.

Figure 6 shows this neutron production rate in terms of the DD contribution to total fusion power in a $f_1 = f_2 = 0.5$ (50:50) D^3He mixture at various well depths. One-half of the DD reactions produce a 2.45 MeV neutron. Note that the DD power fraction never drops below about 0.025 of the total, and that operation at well depth above this minimum will yield increased neutron power. Of course, in the Polywelltm system this can be reduced by changing the fuel mixture ratio, increasing ^3He and decreasing D.

The fusion power goes roughly as $n_D n_{He}$ while the DD (neutron) power goes as $(n_D)^2$, thus the fractional DD neutron power will vary as $n_{He}/n_D = f_2/(1-f_2)$. Reduction of neutron radiation then requires that f_2 be made large (i.e. close to 1.0). If $f_2 = 0.999$, for example, the neutron power will be down by about 1E6 from that of the 50:50 mixture condition and the system will not require any significant radiation shielding. At this level, D^3He is comparable, in terms of radiation hazard, to $p^{11}B$.

However, this mixture is far off of optimum for bremsstrahlung losses, which will be at nearly their maximum possible level — such a system is essentially "all" 3He with $Z = 2$. Applying the previous formalism to this (1:1000) mixture ($f_2 = 0.999$) gives the performance curves shown in Figure 7. From this it is clear that "neutron-free" D^3He systems offer less performance potential than does $p^{11}B$ and, in fact, they can not yield net power at all with any attainable values of F_{BR} .

The utility and potential value of 3He as a fusion fuel thus may be open to question. D competes with it as a neutron-producing fuel, and ^{11}B out-performs it in a "neutron-free" mode. 3He is very scarce and will remain costly even if mined from the lunar surface, while ^{11}B is readily available at reasonable cost on the Earth, and D is found in practically unlimited quantities in all water and is virtually free. However, intermediate D^3He fuel mixtures (e.g. 1:30) allow for a substantial reduction in shielding over DD systems due to the lower neutron rate and run at lower injection energies than comparable $p^{11}B$ systems. Therefore, the use of D^3He in this intermediate range needs to be further explored to determine its true value.

Of course, the power gain scalings given above do not include the power required to supply the B_0 fields, thus they are reasonably correct only for superconducting magnet

systems.^{3*} If magnets are of normal conductors (e.g. copper and/or its alloys) the systems will be driven to still higher injection energies and larger sizes for optimum operation.

Finally, analyses of the systemic effects of synchrotron losses have also been made and are reported elsewhere.⁸ These show optimum operating conditions (i.e. f_1/f_2 mixture fractions and $E_o|_{opt}$) different than those for bremsstrahlung optimization. Since synchrotron radiation will be partially self-absorbed and can be partially reflected, greater flexibility in system design is allowed for its control. For this reason (i.e. it can be made "design-specific") it has not been included here. Bremsstrahlung losses can not be mitigated by system design changes, they are endemic to the plasma mixture, thus are included in the analyses of inherent gain given here.

Studies of the effects of variable D³He mixtures and of magnet drive power requirements are currently underway and will be reported in future EMC2 Technical Notes/Reports.

^{3*} But not exactly, because s/c magnets require cryogenic cooling power for their operation and this power must be included in the power balance for G_{0a} . However, the s/c cooling power is only weakly coupled to the B field strength thus the effect is less profound.

TABLE 1
FUSION CROSS-SECTIONS FOR PARTICLES WITH EQUAL MOMENTUM
 (for E in keV, $\sigma(E)$ in barns)

$$\text{DD:} \quad \sigma(E) = \frac{241}{E[(1.177 - 1.232 \times 10^{-3}E)^2 + 1](e^{23.94/\sqrt{E}} - 1)}$$

$$\text{DT:} \quad \sigma(E) = \frac{147.24 + 18072/[(1.076 - 3.8 \times 10^{-2}E)^2 + 1]}{E(e^{27.57/\sqrt{E}} - 1)}$$

$$\text{D}^3\text{He:} \quad \sigma(E) = \frac{232.92 + 9324/[(1.297 - 1.106 \times 10^{-2}E)^2 + 1]}{E(e^{53.562/\sqrt{E}} - 1)}$$

$$\text{p}^{11}\text{B:} \quad \sigma(E) = \frac{8.4 \times 10^4}{E e^{126.3/\sqrt{E}}} \quad (E < 550 \text{ keV})$$

LIST OF FIGURES

Figure 1. (a-d)

Gross gain in terms of F_{BR} , where $F_{BR} = (B_o R)^4 / r_c$, as a function of electron injection energy, E_o , for the fuels listed in Table 1. Fuel ratios are 50:50, plotted for a range of anode height parameter, $0.01 < \eta < 0.3$.

Figure 1. (e-h)

Gross gain in terms of F_{BR} , where $F_{BR} = (B_o R)^4 / r_c$, as a function of electron injection energy, E_o , for the fuels listed in Table 1. Fuel ratios are for optimum $\langle P_{fb} \rangle$, plotted for a range of anode height parameter, $0.01 < \eta < 0.3$.

Figure 2. (a,b)

System overall gain for DT for anode height parameter $\eta = 0.01$ and 0.1 , plotted as a function of electron injection energy for a range of $F_{BR} = (B_o R)^4 / r_c$, $1E3 < F_{BR} < 1E6$.

Figure 3. (a,b)

System overall gain for DD for anode height parameter $\eta = 0.01$ and 0.1 , plotted as a function of electron injection energy for a range of $F_{BR} = (B_o R)^4 / r_c$, $1E6 < F_{BR} < 1E9$.

Figure 4. (a-d)

System overall gain for D^3He for anode height parameter $\eta = 0.01$ and 0.1 , plotted as a function of electron injection energy for a range of $F_{BR} = (B_o R)^4 / r_c$, $1E6 < F_{BR} < 1E9$ for both 50:50 (a,b) and bremsstrahlung-optimised (c,d) fuel mixtures.

Figure 5. (a-d)

System overall gain for $p^{11}B$ for anode height parameter $\eta = 0.01$ and 0.1 , plotted as a function of electron injection energy for a range of $F_{BR} = (B_o R)^4 / r_c$, $1E8 < F_{BR} < 1E11$ for both 50:50 (a,b) and bremsstrahlung-optimised (c,d) fuel mixtures.

Figure 6.

Percentage of total D^3He fusion power due to DD side reactions as a function of electron injection energy for 50:50 fuel mixture. Plotted for the range of anode height parameter, $0.01 < \eta < 0.3$, used in Figures 1.

Figure 7.

"Neutron-free" D^3He system performance, with $f_2 = 0.999$ ($D:D^3He = 1:1000$).

REFERENCES

- ¹ Bussard, R.W., K.E. King, "Electron Recirculation in Electrostatic Multicusp Systems: II — System Performance Scaling of One-Dimensional 'Rollover' Wells", Energy/Matter Conversion Corporation Report EMC2-0791-04, July 1991
- ² Bussard, R.W., "Ion and Electron Flow and Some Critical Radii in Polywelltm Systems", Energy/Matter Conversion Corporation Report EMC2-0791-02, July 1991
- ³ Bussard, R.W., "Effective Gyro Hole Loss Radius and Diamagnetic Limit in Polywelltm Systems", Energy/Matter Conversion Corporation Report EMC2-0591-02, May 1991
- ⁴ Bussard, R.W., G.P. Jellison, G.E. McClellan, "Preliminary Research Studies of a New Method for Control of Charged Particle Interactions", Pacific-Sierra Research Corp. Report PSR 1899, 30 November 1988, Final Report under Contract DNA001-87-C-0052
- ⁵ Bussard, R.W., K.E. King, "Electron Recirculation in Electrostatic Multicusp Systems: I — Confinement and Losses in Simple Power Law Wells", Energy/Matter Conversion Corporation Report EMC2-0491-03, April 1991
- ⁶ Bussard, R.W., K.E. King, "Virtual Anode Height Variation in Polywelltm Systems", Energy/Matter Conversion Corporation Report EMC2-0991-02, September 1991
- ⁷ Bussard, R.W., K.E. King, "Bremmstrahlung Radiation Losses in Polywelltm Systems", Energy/Matter Conversion Corporation Report EMC2-0891-04, August 1991
- ⁸ Bussard, R.W., K.E. King, "Edge Region Distributions and Synchrotron Radiation", Energy/Matter Conversion Corporation Report EMC2-0991-04, September 1991

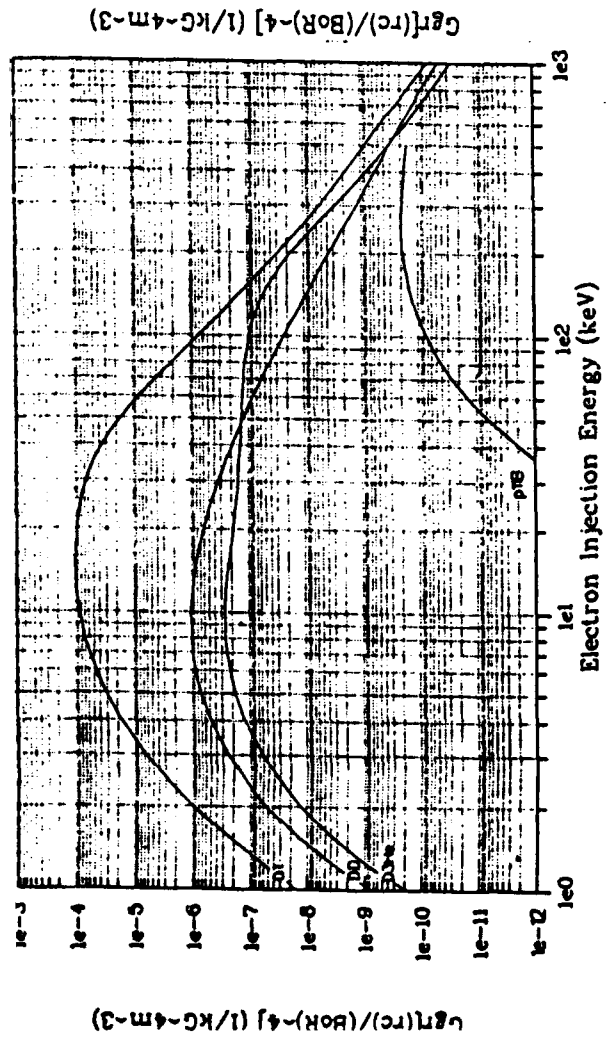


Figure 1 a.

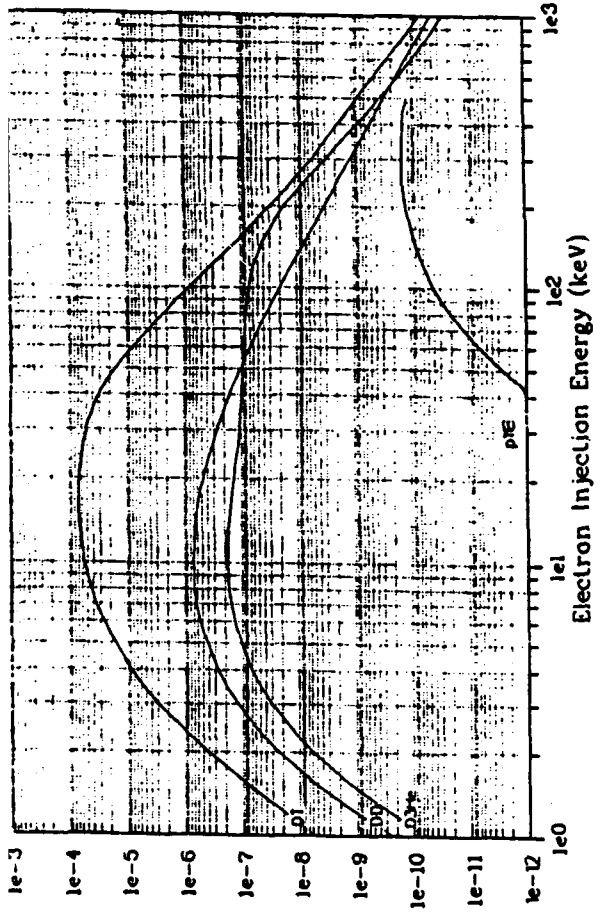


Figure 1 b.

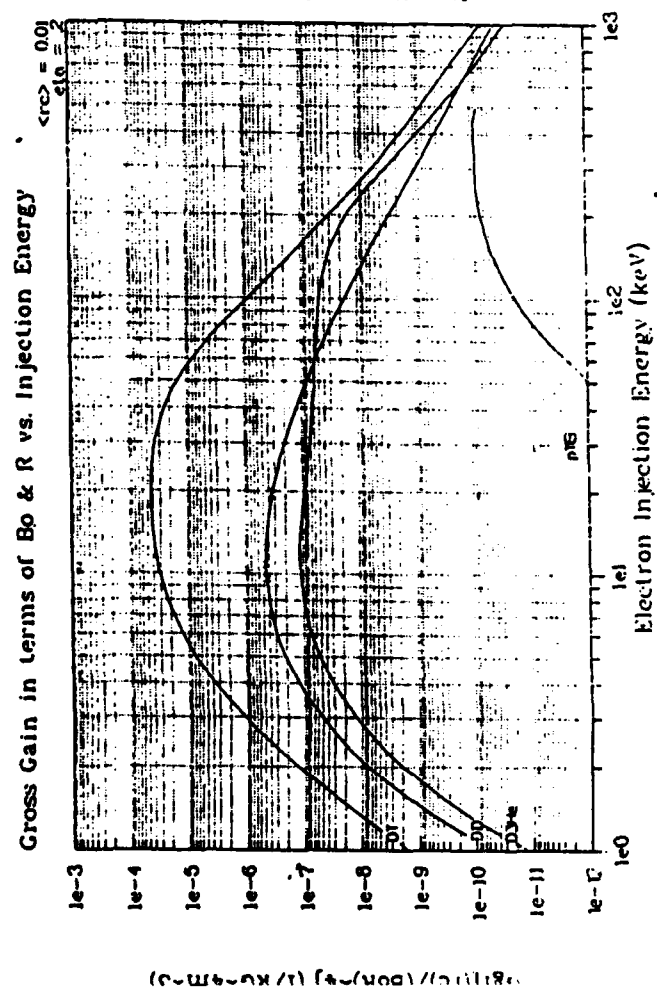


Figure 1 c.

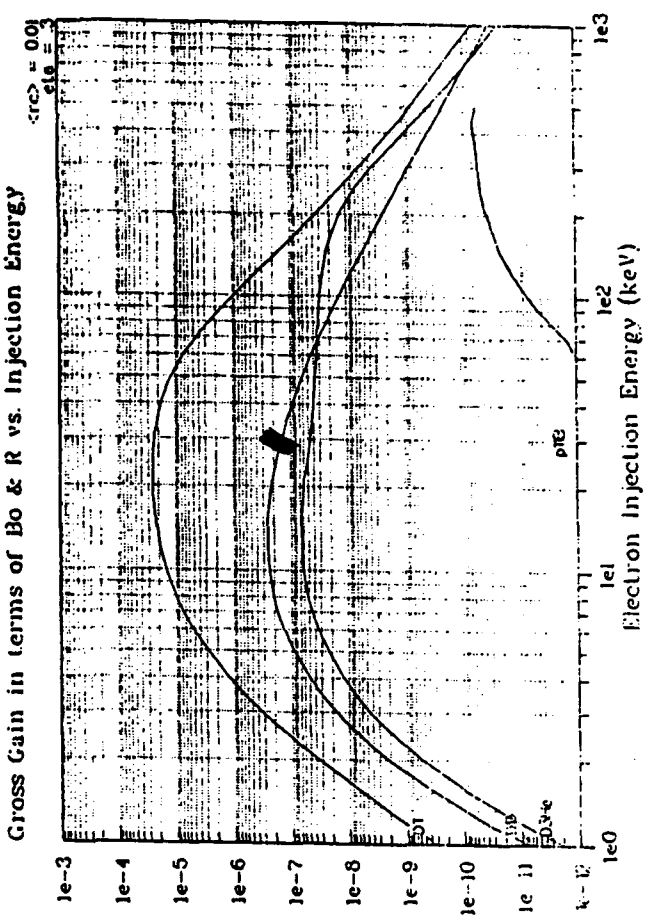


Figure 1 d.

Gross gain in terms of F_{BR} where $F_{BR} = (B_o R)^4 / r_c$, as a function of electron injection energy, E_o , for the fuels listed in Table 1. Fuel ratios are 50:50, plotted for a range of anode height parameter, $0.01 < \eta < 0.3$.

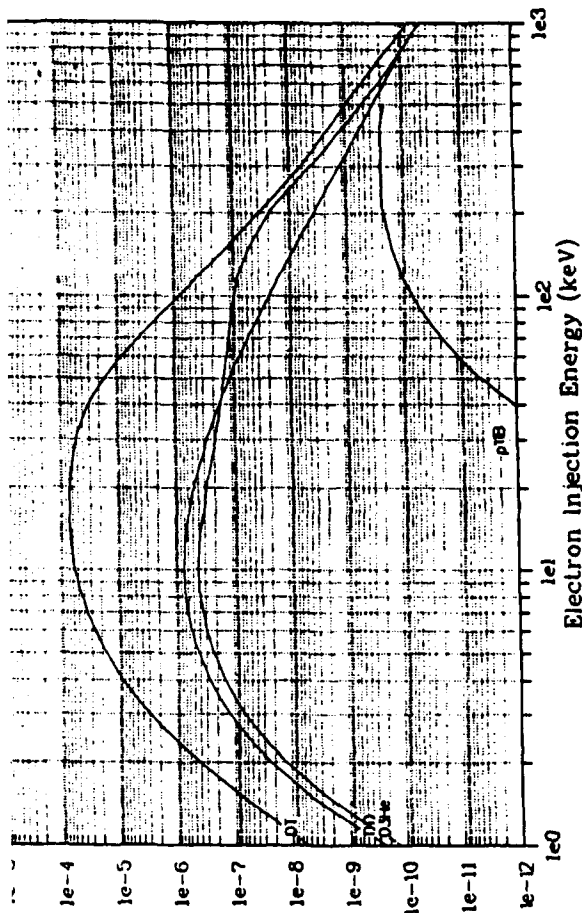


Figure 1 f.

Gross Gain in terms of B_0 & R vs. Injection Energy

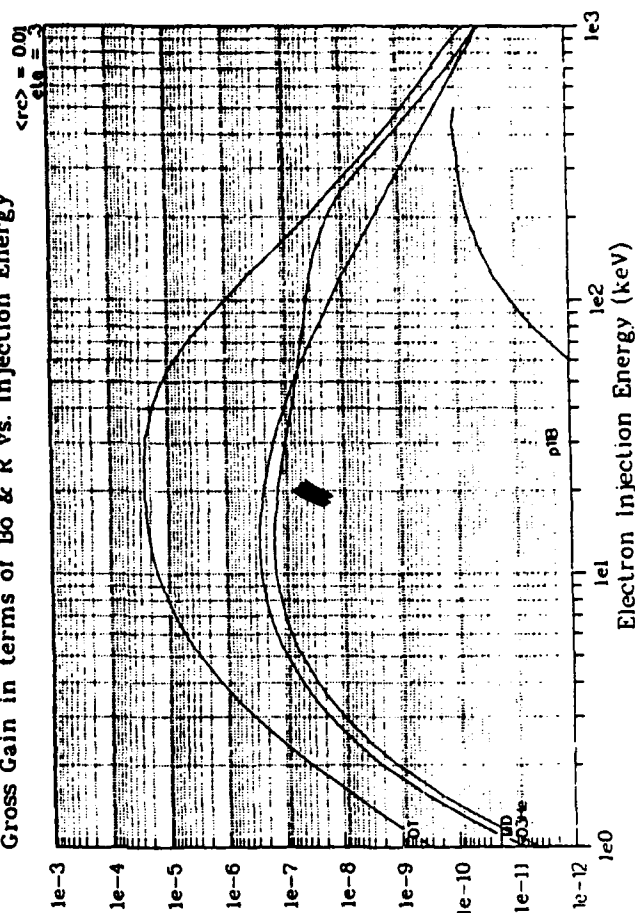


Figure 1 h.

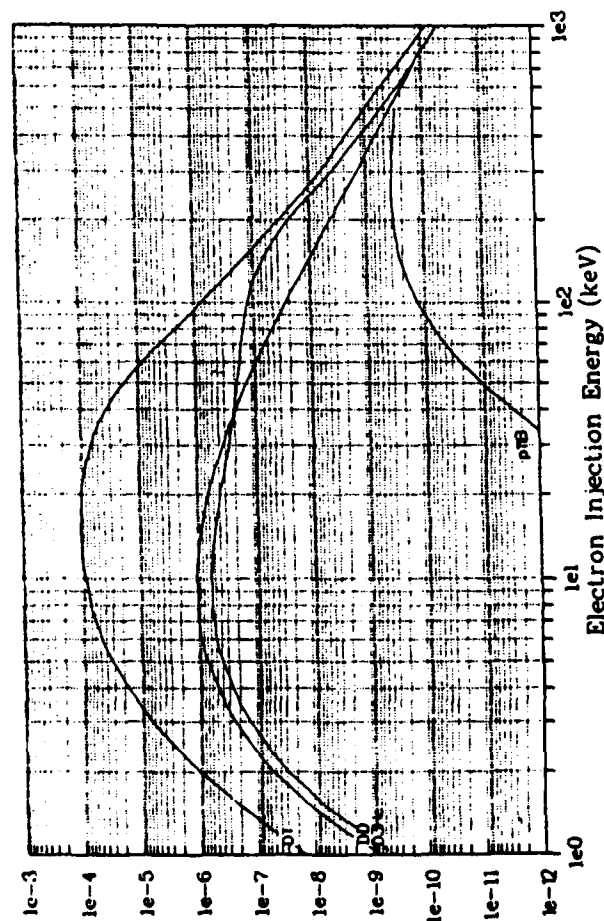


Figure 1 e.

Gross Gain in terms of B_0 & R vs. Injection Energy

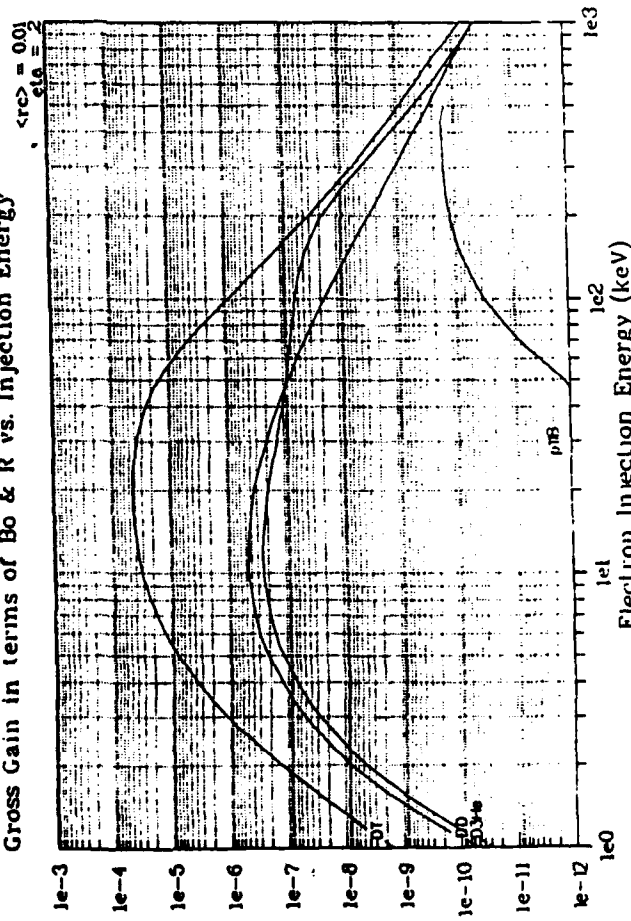


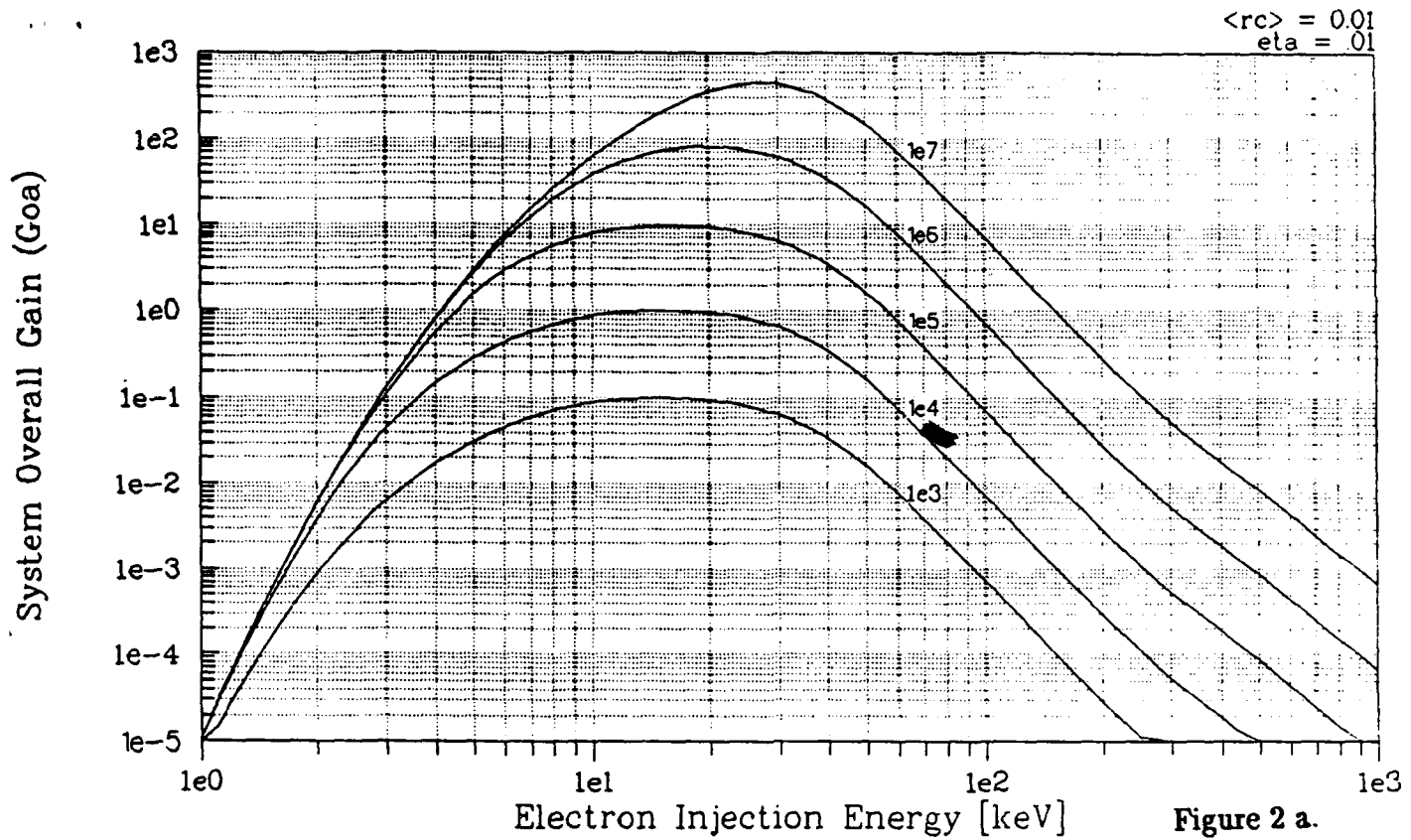
Figure 1 g.

Figure 1. (e-h).

Gross gain in terms of F_{BR} , where $F_{BR} = (B_0 R)^4 / r_c$, as a function of electron injection energy, E_0 , for the fuels listed in Table 1. Fuel ratios are for optimum.

$\langle P_{\eta} \rangle$, plotted for a range of anode height parameter, $0.01 < \eta < 0.3$.

System Overall Gain for DT vs. Injection Energy
for indicated values of $(B_o R)^4 / r_c$ [kG⁴m⁻³]



System Overall Gain for DT vs. Injection Energy
for indicated values of $(B_o R)^4 / r_c$ [kG⁴m⁻³]

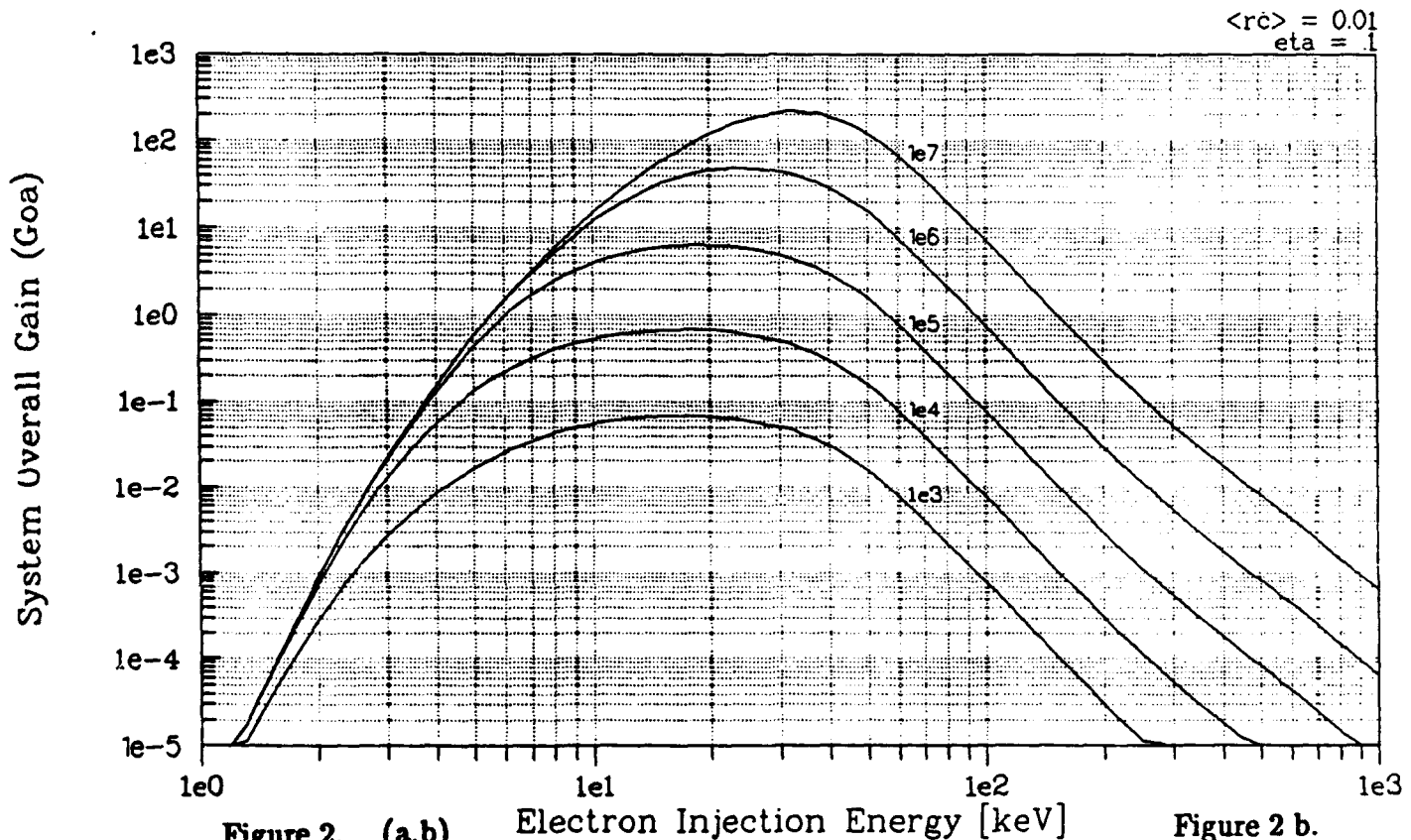


Figure 2. (a,b) Electron Injection Energy [keV]

System overall gain for DT for anode height parameter $\eta = 0.01$ and 0.1 , plotted as a function of electron injection energy for a range of $F_{BR} = (B_o R)^4 / r_c$, $1E3 < F_{BR} < 1E6$.

System Overall Gain for DD vs. Injection Energy
for indicated values of $(B_o R)^4/r_c$ [kG⁴m⁻³]

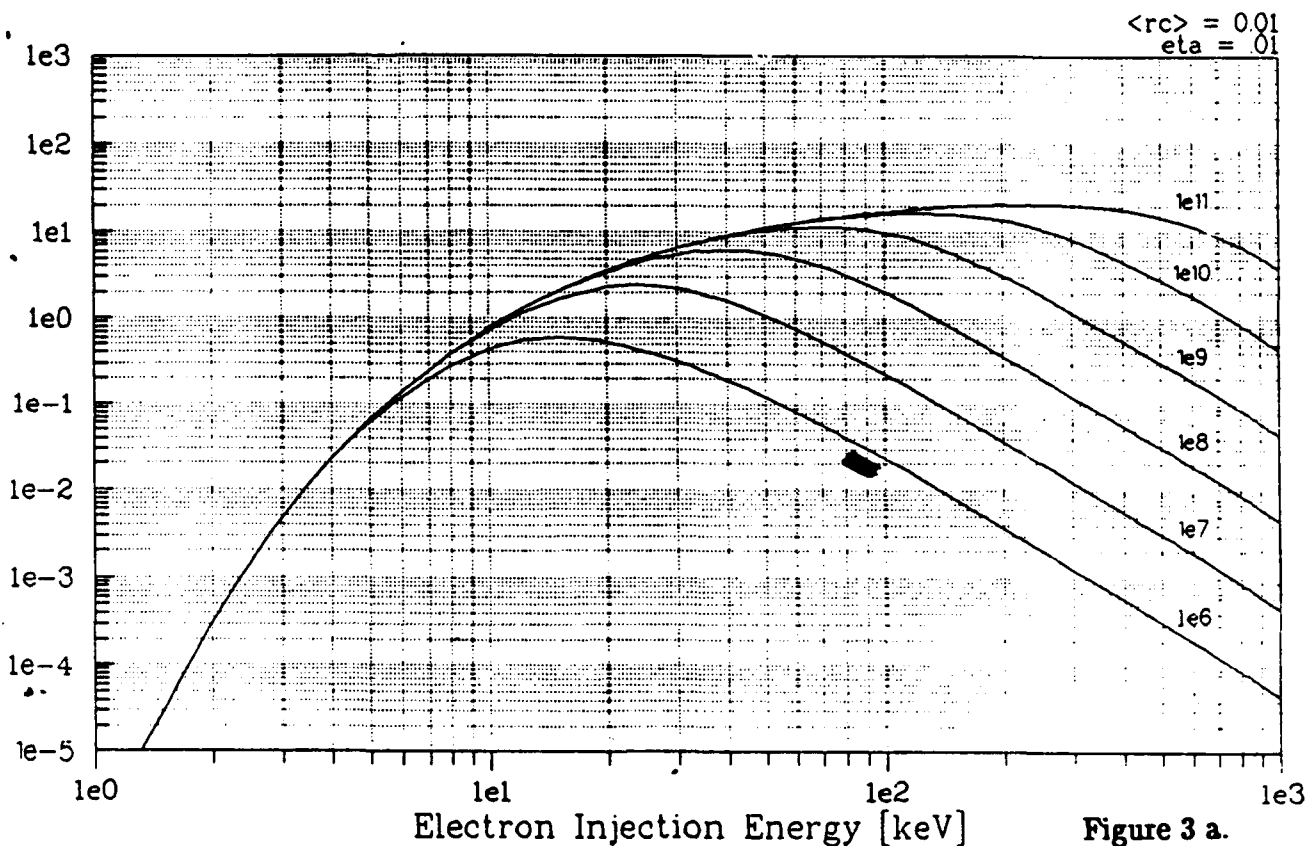


Figure 3 a.

System Overall Gain for DD vs. Injection Energy
for indicated values of $(B_o R)^4/r_c$ [kG⁴m⁻³]

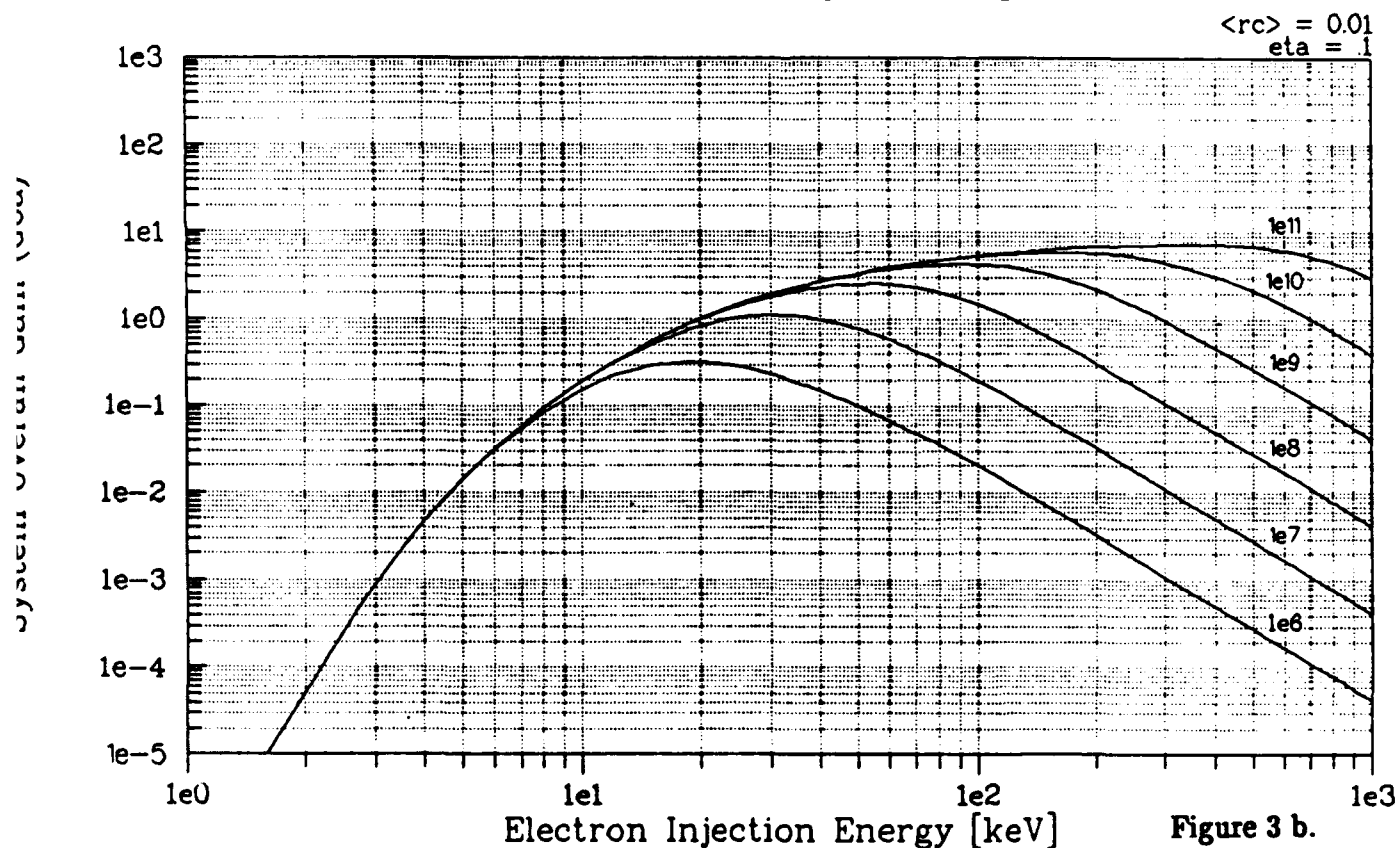


Figure 3 b.

Figure 3. (a,b)

System overall gain for DD for anode height parameter $\eta = 0.01$ and 0.1 , plotted as a function of electron injection energy for a range of $F_{BR} = (B_o R)^4/r_c$,
 $1E6 < F_{BR} < 1E9$.

System Overall Gain for DD vs. Injection Energy
for indicated values of $(B_0 R)^4 / r_c$ [kG⁴m³]

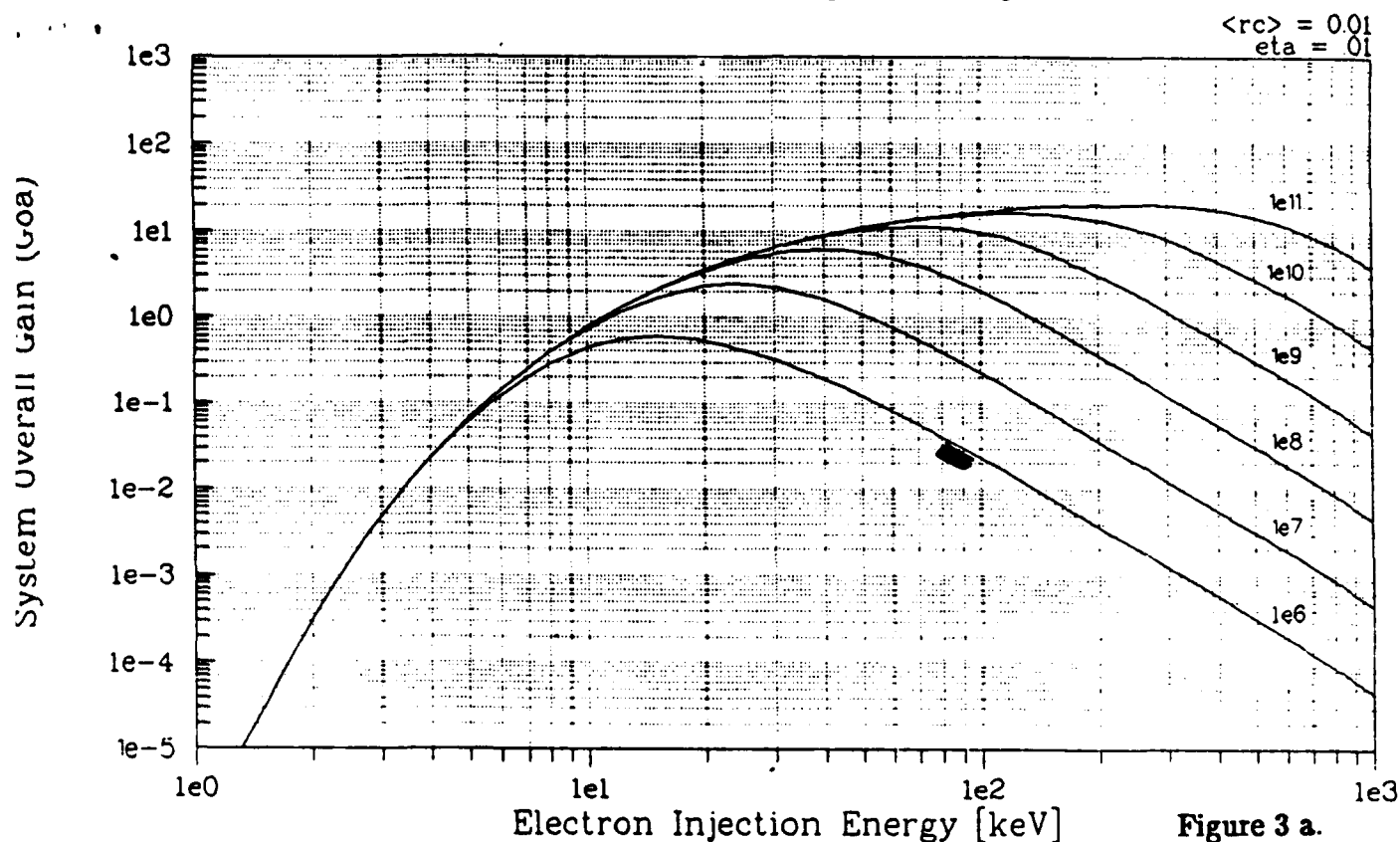


Figure 3 a.

System Overall Gain for DD vs. Injection Energy
for indicated values of $(B_0 R)^4 / r_c$ [kG⁴m³]

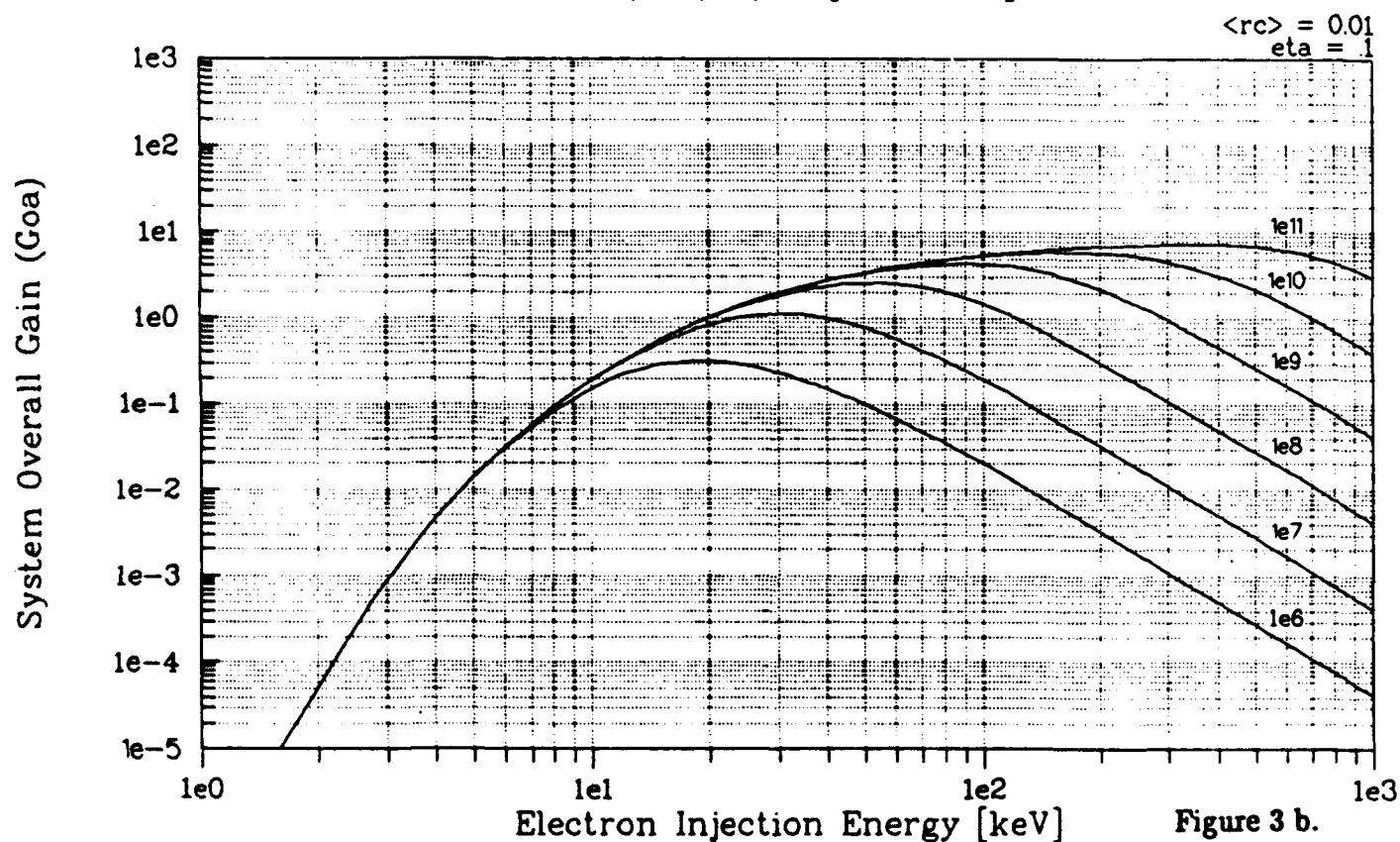


Figure 3 b.

Figure 3. (a,b)

System overall gain for DD for anode height parameter $\eta = 0.01$ and 0.1 , plotted as a function of electron injection energy for a range of $F_{BR} = (B_0 R)^4 / r_c$,
 $1E6 < F_{BR} < 1E9$.

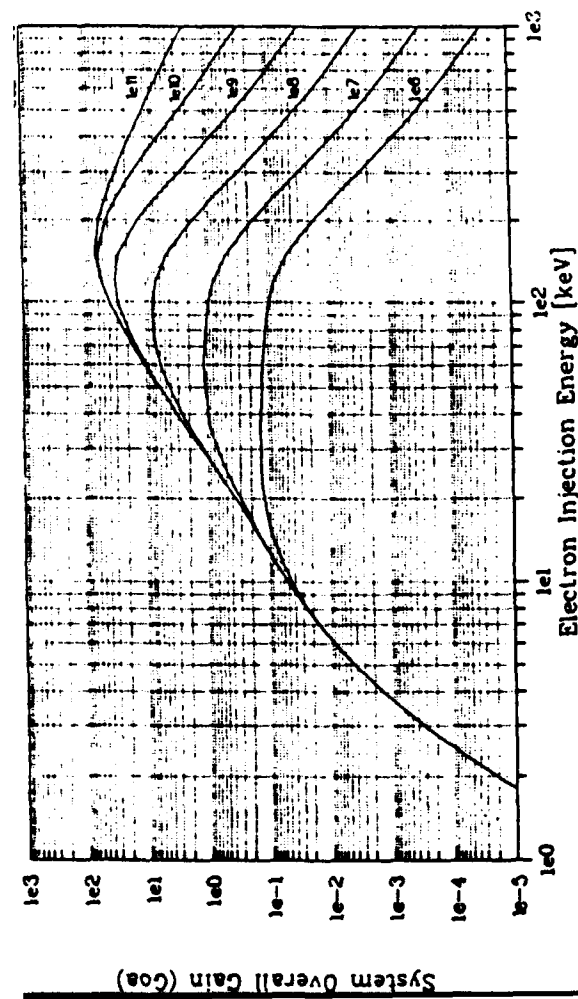


Figure 4 a.

**System Overall Gain for D3He vs. Injection Energy
for indicated values of (BoR)~4/rc [kG~4m~3]**

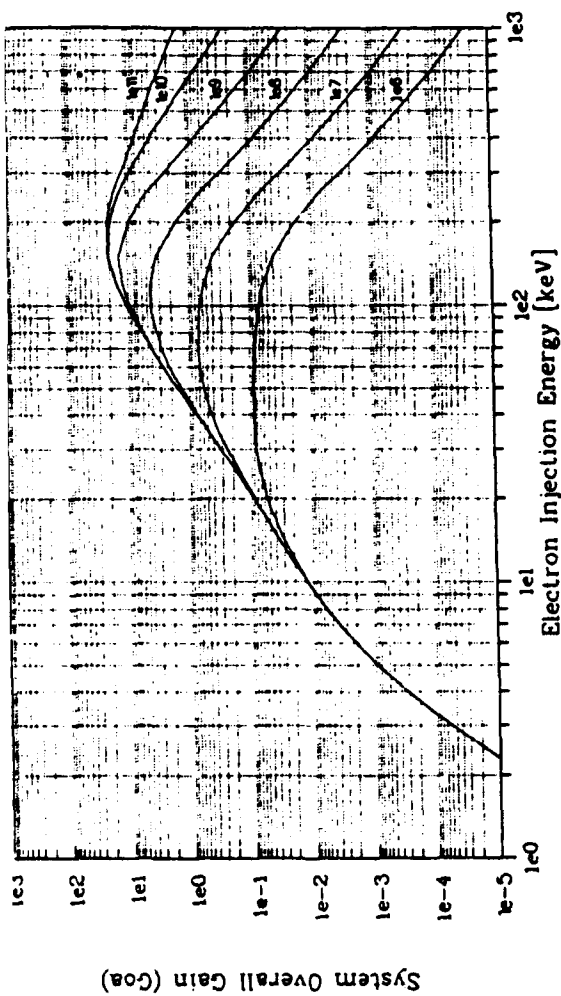


Figure 4 b.

System Overall Gain for D3He vs. Injection Energy for indicated values of $(BoR) \sim 4/rc$ [kG~4m~3]

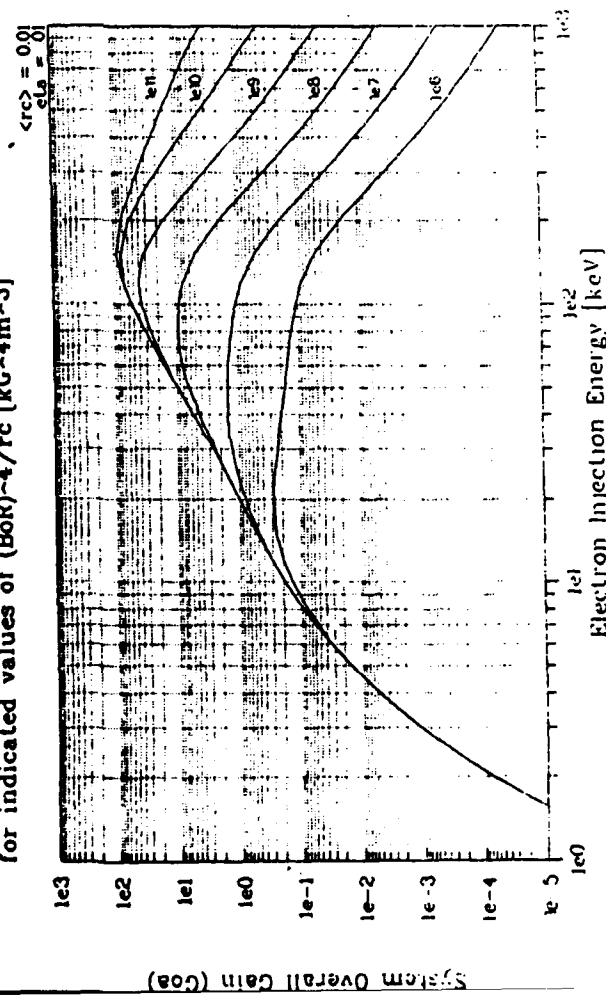


Figure 4 c.

System overall gain for D^3He for anode height parameter $\eta = 0.01$ and 0.1 , plotted

as a function of electron injection energy for a range of $F_{BR} = (B_0 R)^4 / r_c$, $1E6 < F_{BR} < 1E9$ for both 50:50 (a,b) and bremsstrahlung-optimized (c,d) fuel mixtures

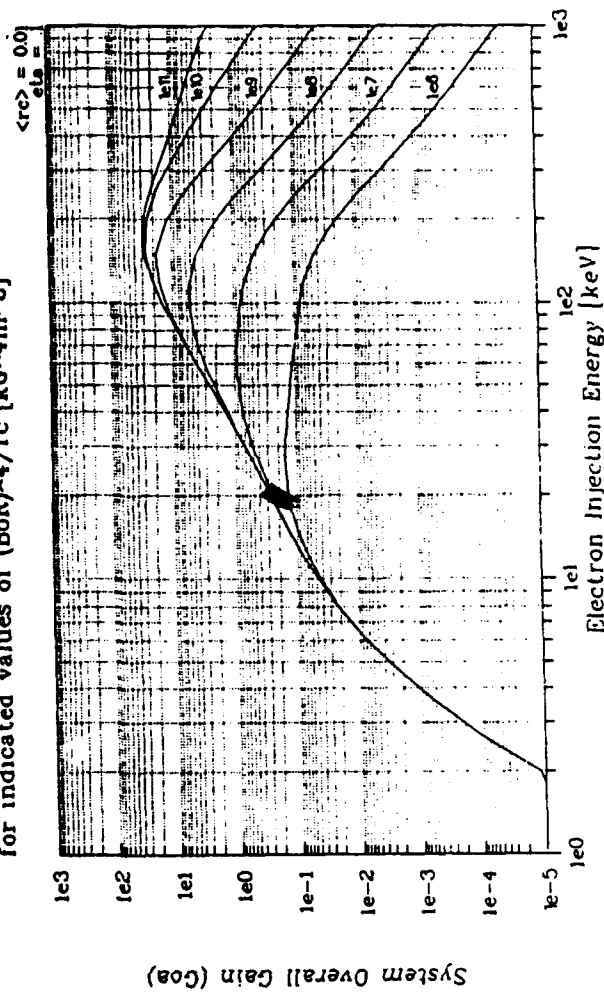


Figure 4 d.

for indicated values of $(BoR)^{-4}/rc$ [kg-4m-3]

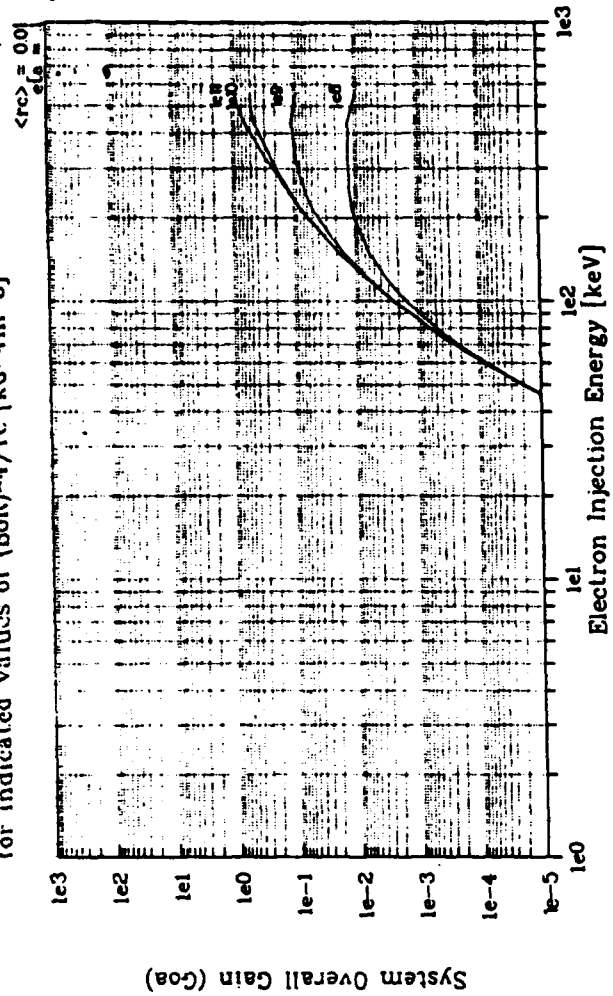


Figure 5 a.

System Overall Gain for p11B vs. Injection Energy for indicated values of $(BoR)^{-4}/rc$ [kg-4m-3]

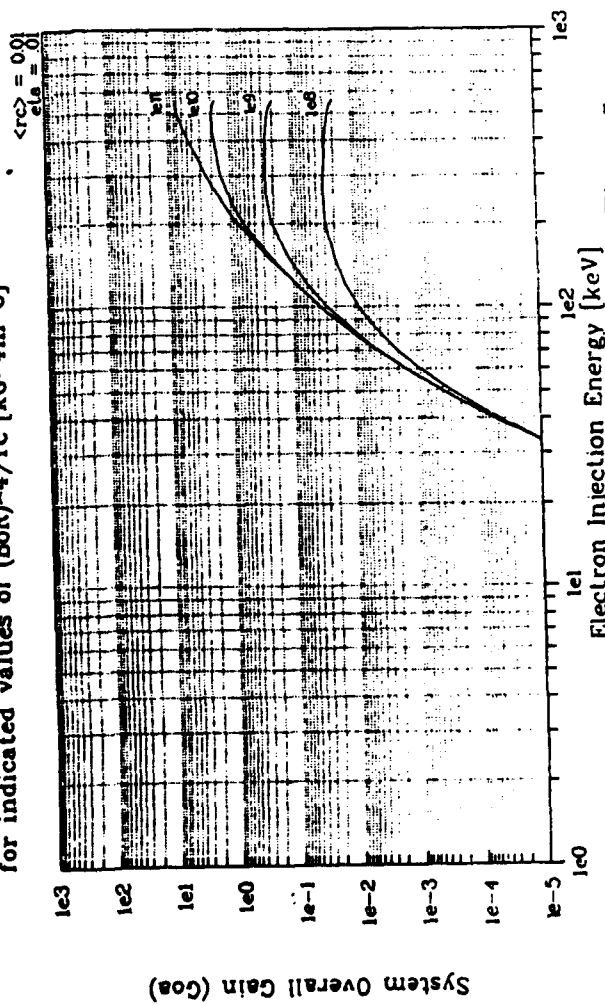


Figure 5 b.

System Overall Gain for p11B vs. Injection Energy for indicated values of $(BoR)^{-4}/rc$ [kg-4m-3]

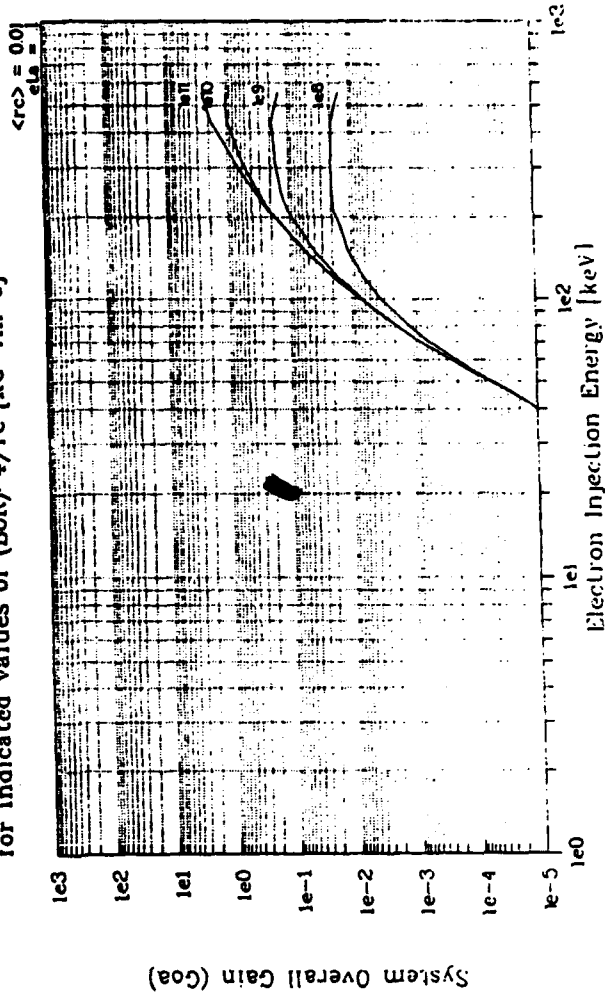


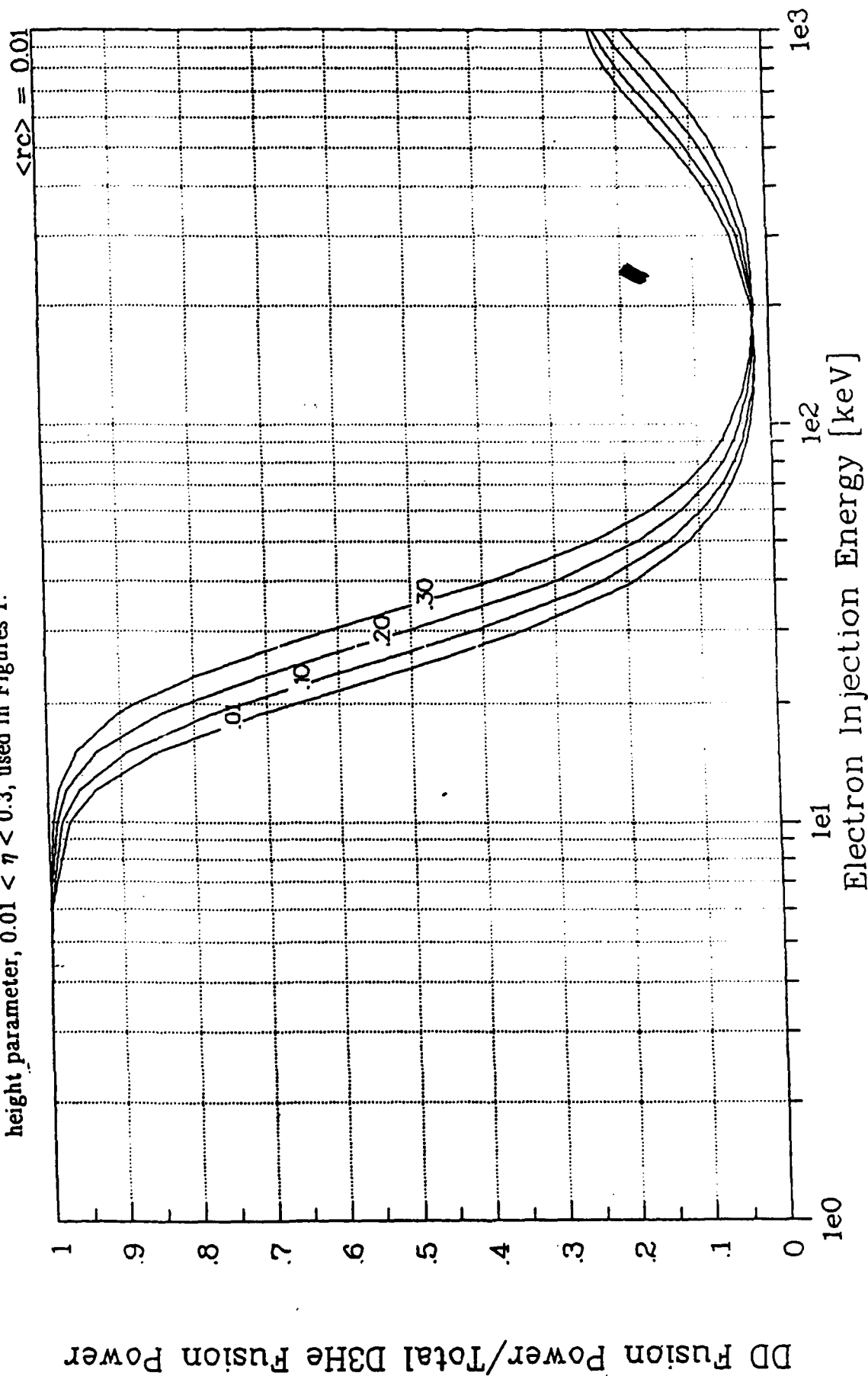
Figure 5 c.

System overall gain for $p^{11}B$ for anode height parameter $\eta = 0.01$ and 0.1 , plotted as a function of electron injection energy for a range of $F_{BR} = (B_o R)^4 / r_c$, $1E8 < F_{BR} < 1E11$ for both 50:50 (a,b) and bremsstrahlung-optimized (c,d) fuel

Figure 5. (a-d)

Figure 6.

Percentage of total D^3He fusion power due to DD side reactions as a function of electron injection energy for 50:50 fuel mixture. Plotted for the range of anode height parameter, $0.01 < \eta < 0.3$, used in Figures 1.



System Overall Gain for D³He vs. Injection Energy
for indicated values of $(BoR) \sim 4/rc$ [kG \sim 4m \sim 3]

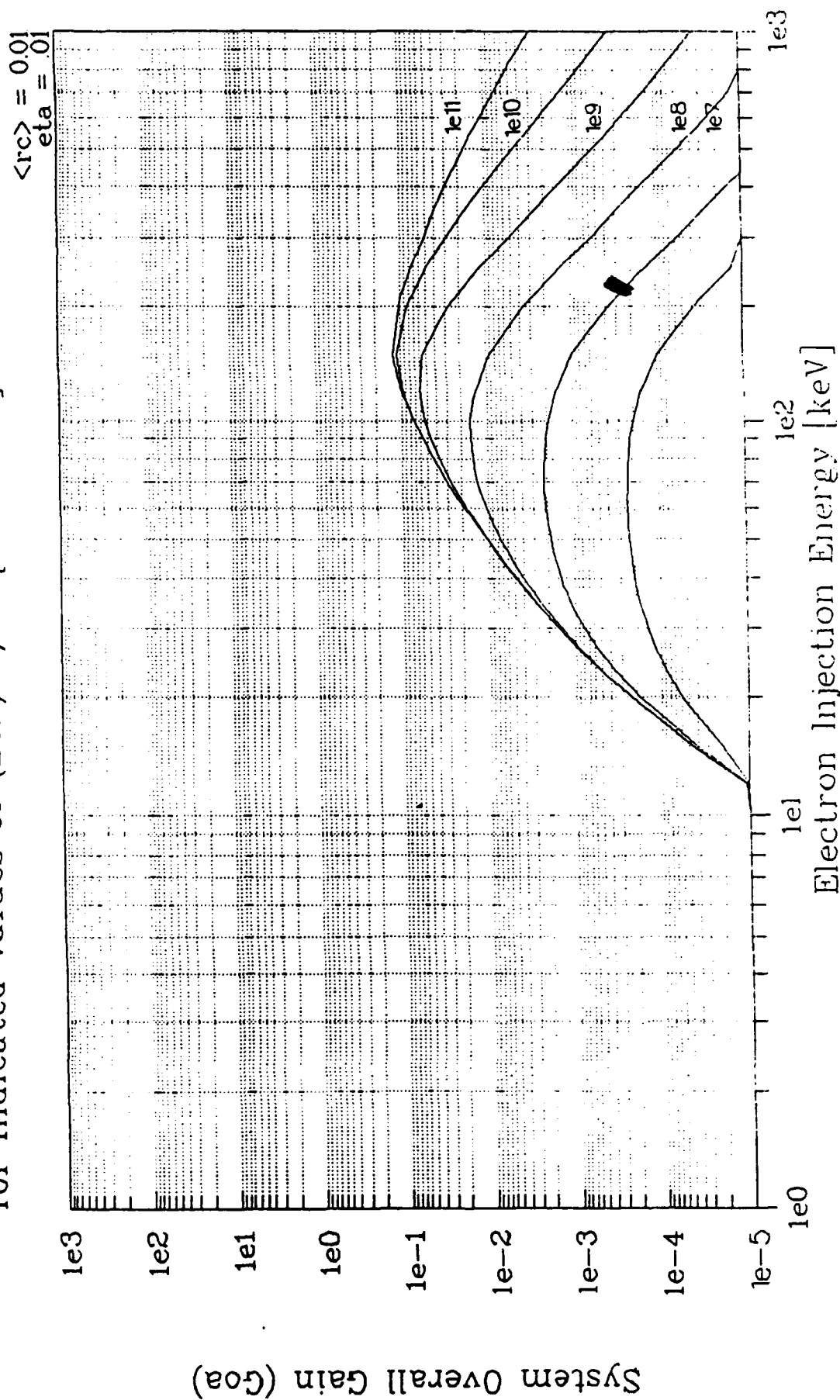


Figure 7.

"Neutron-free" D³He system performance, with $f_2 = 0.999$ (D:³He = 1:1000).